Biosensors and Bioelectronics 29 (2011) 189–194

Contents lists available at SciVerse ScienceDirect

Biosensors and Bioelectronics

journal homepage: www.elsevier.com/locate/bios

A biomimetic sensor for the determination of extracellular O_2^- using synthesized Mn-TPAA on TiO_2 nanoneedle film

Yongping Luo, Guoqi Hu, Anwei Zhu, Biao Kong, Zhen Wang, Chunyuan Liu, Yang Tian*

State Key Laboratory of Pollution Control and Resources Reuse, Department of Chemistry, Tongji University, Siping Road 1239, Shanghai 200092, PR China

ARTICLE INFO

Article history:
Received 14 June 2011
Received in revised form 12 August 2011
Accepted 14 August 2011
Available online 22 August 2011

Keywords:
Biomimetic sensor
Superoxide ion
Mn-TPAA
TiO_2 nanoneedles
Living cells

ABSTRACT

By immobilizing synthesized Mn-TPAA (TPAA = tris[2-[*N*-(2-pyridylmethyl) amino] ethyl] amine) on TiO_2 nanoneedle surface, a biosensor for superoxide ion (O_2^-) has been developed and applied for determination of O_2^- released from living cells. Direct electron transfer of Mn-TPAA is realized with a formal redox potential ($E^{\circ\prime}$) falling in the range of the $E^{\circ\prime}$ values of the redox couples O_2/O_2^- and O_2^-/H_2O_2. This suggests that Mn-TPAA on TiO_2 films is electrochemically active and capable of thermodynamically mediating both the oxidation of O_2^- to O_2 and the reduction of O_2^- to H_2O_2. Therefore, Mn-TPAA immobilized on the TiO_2 films can be used electrochemically for determination of O_2^- due to its electrochemical activities and biomimetic catalytic activities like superoxide dismutase (SOD) toward O_2^-. The present biomimetic O_2^- sensor shows high selectivity at the low working potential of 0 V vs. Ag|AgCl, a wide linear range from 10^{-7} M to 10^{-4} M and a quick response time within 6 s. By taking advantage of the developed method and the properties of biomimetic SOD themselves, we have realized the real-time monitoring of O_2^- concentration released from living cells and investigated the relationship between the concentration changes of O_2^- and intracelluar Ca^{2+}, which may gain additional insights on the reactive oxygen species (ROS) signal transduction and other physiological and pathological events.

1. Introduction

Reactive oxygen species (ROS) are a class of highly reactive reduced oxygen molecules, including superoxide anion (O_2^-), hydroxyl radical (HO•), hydrogen peroxide (H_2O_2), and so on. The primary species of ROS-O_2^- has relatively low concentration under normal physiological condition, because it undergoes a process termed dismutation or disproportionation by superoxide dismutase (SOD) to form H_2O_2 and O_2 (McCord and Fridovich, 1968). However, in some cases, for example, traumatic brain injury, ischemia–reperfusion and hypoxia, the concentration of O_2^- would significantly increase (Kontos and Wei, 1986; Thomas et al., 1996; Ellis et al., 2008; Ji et al., 2009; Wrona and Dryhurst, 1998; Sadek et al., 2004; Globus et al., 1995; McCord and Fridovich, 1969; Komatsu et al., 2009). It is considered that O_2^- may be involved in the etiology of aging, cancer, and progressive neurodegenerative damage such as Parkinson's disease (Mossine et al., 1999; Hall and Braughler, 1989; Vanella et al., 1993; Floyd, 1990; Wang et al., 2008; Barroso et al., 2011). Unfortunately, the detailed mechanism of O_2^--triggered diseases and the route of O_2^--induced ROS signal transduction are still unclear. It has ever been reported that as a charged and short-lived anion, superoxide anion O_2^- is insufficient to indicate intracellular signalling due to the combination of a poor permeability through the phospholipid bilayer and a rapid dismutation to uncharged and more stable derivative, H_2O_2 (Tanabe et al., 2005; Finkel, 2003). But, recent evidence has indicated that extracellular O_2^-, not H_2O_2, leads to Ca^{2+} signalling and apoptosis in pulmonary endothelial cells (Hawkins et al., 2007). Anyway, the difficulties in opening up the mechanism of O_2^--induced oxidative stress and subsequent diseases originate from the properties of O_2^- including relatively high reactivity, short life-time, and varying concentrations in broad range. Thus, it is still a challenging work to establish a reliable and durable approach for real-time determination of O_2^-, which may facilitate the investigation on the physiological and pathological processes related to O_2^- and other ROS.

Over the past decades, several elegant methods have been developed for the determination of O_2^- with high sensitivity and selectivity, such as EPR spin trapping, chemiluminescence, and electrochemical measurements (Li et al., 2009; Xu et al., 2007; Tang et al., 2008; Ohara et al., 1993; Vasquez-Vivar et al., 1997; Ohyashiki et al., 1999; Mason and Knecht, 1994; Shi et al., 2007; Ai et al., 2005). Electrochemical approaches have attracted more attention because of simplicity, low instrumental cost, and capability in real time, and even *in vivo* detection (Ohsaka et al., 2002). A large number of papers have been published on the electrochemical determination of O_2^- (Mesároš et al., 1998; Song et al., 1995; McNeil et al., 1992; Lvovich and Scheeline, 1997; Wang et al., 2009;

* Corresponding author. Tel.: +86 21 65987075; fax: +86 21 65981097.
E-mail address: yangtian@mail.tongji.edu.cn (Y. Tian).

0956-5663/$ – see front matter © 2011 Elsevier B.V. All rights reserved.
doi:10.1016/j.bios.2011.08.017

Di et al., 2004; Tian et al., 2002, 2004, 2005; Liu et al., 2008; Deng et al., 2008), typically based on the incorporation of enzymes onto electrodes for improving the selectivity of $O_2^{-\bullet}$ biosensors. The two main enzymes employed in the construction of O_2^- biosensor are cytochrome (cyt *c*) and SOD. The SOD-based O_2^- biosensors have paved an elegant way for assay of $O_2^{-\bullet}$ with high selectivity and low detection limit because SOD is the specific enzyme for the dismutation of O_2^- (Song et al., 1995).

The research interest in ROS motivates us to further develop O_2^- biosensors on the basis of biomimetic enzymes, which are expected to have higher stability and better reproducibility than natural enzymes, and have the selectivity and sensitivity in O_2^- detection comparable with those of SOD. Recently, we reported a facile strategy with high selectivity and stability for monitoring O_2^- through direct electron transfer of manganese (II) phosphate ($Mn_3(PO_4)_2$) (Luo et al., 2009; Zhou et al., 2011). In the present work, Mn-TPAA was used for O_2^- detection. With a formal redox potential ($E^{\circ\prime}$) located between the $E^{\circ\prime}$ values of the redox couples O_2/O_2^- and O_2^-/H_2O_2, which are reported to be −330 mV and +940 mV vs. NHE, respectively (Bard et al., 1985; Hai, 2006), direct electron transfer of Mn-TPAA was observed on the TiO_2 nanoneedle film surface. Experimental data demonstrated that Mn-TPAA was stably confined onto the TiO_2 surfaces. By immobilizing Mn-TPAA on the TiO_2 films, a new electrochemical approach for determination of O_2^- was developed, because the biocatalytic activities of Mn-TPAA toward O_2^- were reported (Deroche et al., 1996). The method was found to be reliable and durable and had high selectivity, broad linear range, and quick response time. The good analytical performance as well as the advantages of biomimetic SOD provided a platform to real-time determination of O_2^- released from living cells. The relationship between O_2^- and Ca^{2+}, which might influence the ROS signal transduction and other physiological and pathological events, was further studied by employing the new method.

2. Experimental

2.1. Chemicals and materials

2-Pyridinecarboxaldehyde, uric acid (UA), ascorbic acid (AA), dopamine (DA), L-cysteine (Cys), and sodium molybdenum oxide dihydrate were obtained from Alfa Aesar. 4,4′-Diisothiocyanatostilbene-2,2′-disul (DIDS), angiotensin II (Ang II), apocynin (Apo), Na–HEPES, bovine serum albumin (BSA), sulfinpyrazone, pluronic® F-127, and fetal bovine serum (FBS) were purchased from Sigma–Aldrich. Fluo 4-AM was purchased from Dojindo Laboratory (Kumamoto, Japan). Iron(II) chloride tetrahydrate was obtained from Adamas Reagent Co., Ltd. Phosphate buffer solution (PBS) was prepared by mixed stock standard K_2HPO_4 and KH_2PO_4 solutions (Sinopharm Chemical Reagent Co., Ltd.) and pH of PBS was adjusted by pH meter. A stock solution of KO_2 was prepared by adding KO_2 to dimethyl sulphoxide (DMSO) which stored together with molecular sieve 4 Å (Wako Pure Chemical Industries, Ltd.), sonicating the solution for 5 min. The chemical generation of O_2^- was performed by dissolving KO_2 in DMSO solution (Islam et al., 2009; Oritani et al., 2004). The concentration of O_2^- was measured by recording the reduction of ferricytochrome *c* spectrophotometrically with an Agilent 8453 UV–vis–NIR spectrophotometer (Agilent Instruments, USA) and using the extinction coefficient (21.1 $mM^{-1}\,cm^{-1}$) of ferrocytochrome *c* at 550 nm (Fridovich, 1970; Liu et al., 2008). Singlet oxygen ($^1O_2$) was generated as a product of the disproportionation of H_2O_2 in 10 mM PBS (pH 10.5) catalyzed by sodium molybdenum oxide dehydrate. Hydroxyl radical ($HO^\bullet$) was generated in 10 mM PBS (pH 4.0) catalyzed by Fe^{2+} (Fenton Reaction). Other reagents were of analytical grade. All aqueous solutions were prepared with double distilled water. Indium tin oxide (ITO) glass plates with a square resistance of 10–20 $\Omega\,cm^{-2}$ were obtained from Shenzhen Nanbo Display Technology Co., Ltd. (Shenzhen, China).

2.2. Synthesis of Mn-TPAA

TPAA was synthesized according to the previous method (Nagano et al., 1989). In brief, 2-pyridinecarboxaldehyde (1.61 g) was added into a stirred solution of 15 mL of anhydrous methanol containing tris(2-aminoethyl)-amine (0.73 g). The stirred mixture was refluxed with 3 Å molecular sieves under an argon atmosphere and in the dark. After 3 h, the Schiff base in the solution was reduced by $NaBH_4$, and the reaction mixture was stirred overnight at room temperature. Then the solvent was evaporated after filtering out the molecular sieves, and an aqueous saturated K_2CO_3 solution was added. The compound was extracted with CH_2Cl_2 (3× 25 mL), and the organic layer was dried over anhydrous $MgSO_4$. Then, the solvent was evaporated to form a yellow oil of TPAA (1.68 g). Finally, $MnCl_2$ aqueous solution was added to the methanol solution of TPAA at room temperature, and the reaction mixture was keeping for 5 min at room temperature. The solvent was then thoroughly removed to form Mn-TPAA.

2.3. Preparation and modification of TiO_2 film

ITO-coated glass plates were thoroughly cleaned by sonication for 20 min in the following solutions successively: neat ethanol, 1 M NaOH at 60 °C, and distilled de-ionized water. The TiO_2 nanoneedle sol (Ishihara Sangyo Kaisha, Ltd., Japan) was coated onto ITO-coated glass by spin-coating method, and annealed at 723 K for 1 h. Then the mixtures of 0.5 M TiO_2 nanoneedles and 8.21×10^{-4} mol/g TPAA (or 7.88×10^{-4} mol/g Mn-TPAA) sol were covered onto the surface of TiO_2 nanoneedle film by spin-coating method and dried at 373 K to form a TPAA or Mn-TPAA modified TiO_2 film, which will be noted as TPAA/TiO_2 or Mn-TPAA/TiO_2 film hereafter, respectively. The thickness of TPAA/TiO_2 or Mn-TPAA/TiO_2 film is about 5 μm. The ratio of TPAA or Mn-TPAA to TiO_2 is 1:10. The optimized dimension of electrode was determined to be ~1.0 cm × 0.2 cm. The electrodes were kept dry in room temperature when no use.

2.4. Apparatus and measurements

All electrochemical measurements were performed with a CHI 660 electrochemical work station (Chenhua, Shanghai). TPAA/TiO_2 or Mn-TPAA/TiO_2 film was employed as the working electrode. The reference electrode was a KCl-saturated Ag|AgCl electrode, while the auxiliary electrode was a platinum wire. Prior to experiment, solution was bubbled with purified nitrogen for at least 30 min to remove oxygen.

2.5. Detection of extracellular O_2^- generated from the stimulus of Ang II

The HeLa cells were obtained from School of Life Sciences and Technology, Tongji University, Shanghai, China. HeLa cells were cultured in Dulbecco's Modified Eagle's medium (DMEM) supplemented with 10% fetal bovine serum (FBS), 100 units mL^{-1} penicillin, and 100 μg mL^{-1} streptomycin at 37 °C in a humidified atmosphere of 95% air with 5% CO_2. The HeLa cells were suspended in 10 mM PBS (pH 7.4) at a concentration of 5×10^5 cells mL^{-1} for electrochemical and fluorescent measurements. The electrochemical responses were recorded at a Mn-TPAA/TiO_2 electrode stimulated without or with 2 μM Ang II in 10 mM PBS (pH 7.4) con-

taining suspended living cells and 100 mM glucose at the applied potential of 0 mV vs. Ag|AgCl.

2.6. Imaging of Ca^{2+} in cells

HeLa cells cultured in a tissue culture dish were loaded with the cytosolic Ca^{2+} indicator Fluo 4-AM (5 μM) (Morton-Jones et al., 2008; Erriquez et al., 2009) at room temperature for 30 min in extracellular medium (ECM) containing 121 mM NaCl, 5 mM $NaHCO_3$, 10 mM Na–HEPES, 4.7 mM KCl, 1.2 mM KH_2PO_4, 1.2 mM $MgSO_4$, 2 mM $CaCl_2$, 10 mM glucose, and 2.0% bovine serum albumin (BSA), pH 7.4, in the presence of 100 μM sulfinpyrazone and 0.003% pluronic® F-127. The cells were washed and resuspended in the experimental imaging solution (ECM containing 0.25% BSA). After the cells were stimulated with 2 μM Ang II, confocal fluorescence imaging was performed with an OLYMPUS FV1000 laser scanning microscope and a 60× oil-immersion objective lens. Cells loaded with dyes were excited at 488 nm using an Ar laser. Emission was collected from 500 to 600 nm. For inhibitor studies, the NADPH oxidase inhibitor Apo (2 μM) and the anion channel blocker DIDS (300 μM) were added for 10 min before the above experiment. Quantitation by line plots was analyzed using the software package provided by Olympus Instruments. The relative fluorescence intensity of Ca^{2+} concentrations in the cells was obtained in three selected independent fields. Quantitation of Ca^{2+} concentrations in the cells was expressed as fold change vs. baseline (zero time).

3. Results and discussion

3.1. Electrochemical properties of Mn-TPAA/TiO_2 films

Electrochemical behaviors of Mn-TPAA were investigated. As depicted in Fig. 1, a couple of stable and well-defined redox peaks were observed at Mn-TPAA/TiO_2, whereas no peaks were obtained at either TPAA/TiO_2 film or bare TiO_2 nanoneedle film within the same potential scan ranges. The formal potentials ($E^{\circ\prime}$) of Mn-TPAA/TiO_2 was estimated to be 622.8 ± 2.5 mV vs. Ag|AgCl. The value is located between the $E^{\circ\prime}$ values of the O_2/O_2^- and O_2^-/H_2O_2 redox couples (Bard et al., 1985; Hai, 2006). Thus, Mn-TPAA/TiO_2 film is thermodynamically capable of mediating both the oxidation of O_2^- to O_2 and the reduction of O_2^- to H_2O_2.

Cyclic voltammograms (CVs) obtained at Mn-TPAA/TiO_2 film at different scan rates in 10 mM PBS (pH 7.0) containing no Mn-TPAA are given in Supporting Information, Fig. S1. Both cathodic and anodic peak current densities (J_p^a and J_p^c) are in linear relationship with the scan rates in the potential scan range from 10 to 500 mV s^{-1}. It suggests that the electrochemical processes are surface-controlled. In addition, the CVs remained essentially unchanged on consecutive potential scanning in fresh PBS without Mn-TPAA, up to 2000 cycles at sweep rate of 50 mV s^{-1}, indicating that Mn-TPAA was very stable after immobilized on the TiO_2 nanoneedle film. According to Laviron's procedure (Laviron, 1979), the relevant kinetic parameters of the electrode reaction, i.e. the rate constant of the electrochemical process (k_s) and cathodic transfer coefficients (α_c), were estimated to be 0.69 s^{-1} and 0.47, respectively.

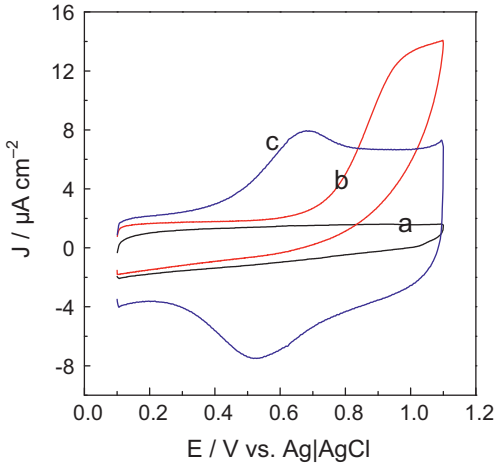

Fig. 1. CVs obtained at (a) bare TiO_2 film, (b) TPAA/TiO_2 film, and (c) Mn-TPAA/TiO_2 film in 10 mM PBS (pH 7.0). Potential scan rate: 50 mV s^{-1}.

3.2. Electrocatalytic activity toward O_2^-

As described above, Mn-TPAA was stably immobilized on the TiO_2 nanoneedle film and direct electron transfer of Mn-TPAA was facilitated by the TiO_2 nanoneedles. The combination of direct electron transfer and the biocatalytic activity of Mn-TPAA toward O_2^- provided a reliable platform for the determination of O_2^- anodically or cathodically. The electrocatalytic activity of Mn-TPAA/TiO_2 electrodes toward O_2^- was first investigated by cyclic voltammetry. Fig. 2 shows typical CVs obtained at Mn-TPAA/TiO_2 film in 10 mM PBS (pH 7.0) in the absence of O_2^- (a) and presence of (b) 1 mM and (c) 3 mM O_2^-. CVs of TPAA and bare TiO_2 nanoneedle film in the presence of O_2^- were also given for comparison. Both anodic and cathodic peaks in the potential range of ~0.4–0.7 V vs. Ag|AgCl increased with the increasing concentration of O_2^- at Mn-TPAA/TiO_2 electrodes, while no response was obtained at bare TiO_2 film and TPAA/TiO_2 film at the same potential range after the addition of O_2^- with the same concentration. These results indicate that the increased peak currents are ascribed to the mediation of Mn-TPAA for the dismutation of O_2^-. Thus, we can determine O_2^- either anodically or cathodically by amperometric method.

Fig. 3 shows a typical amperometric response of Mn-TPAA/TiO_2 film toward O_2^-. A large anodic (A) or cathodic (B) current was clearly observed at Mn-TPAA/TiO_2 electrode at +650 mV or 0 mV when KO_2 was injected into the solution to generate O_2^-. However, relatively small responses were obtained at the bare TiO_2 film and TPAA/TiO_2 film toward the same concentration of O_2^-.

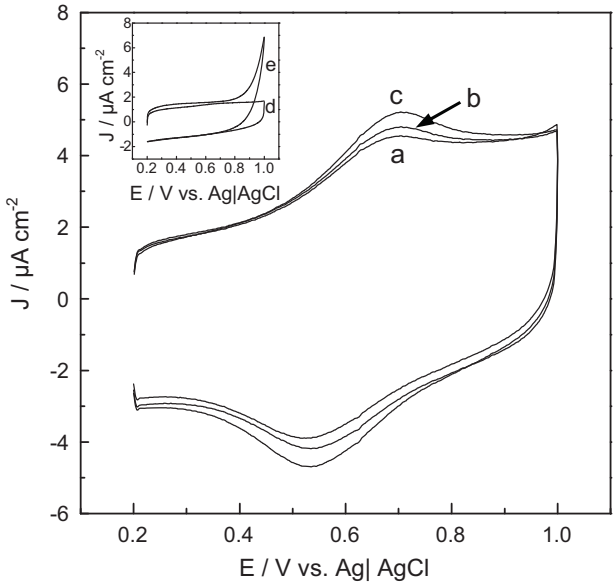

Fig. 2. CVs obtained at Mn-TPAA/TiO_2 film in 10 mM PBS (pH 7.0) in the absence (a) and presence of (b) 1 mM and (c) 3 mM O_2^-. The inset shows the CVs of (d) bare TiO_2 film and (e) TPAA/TiO_2 film in the presence of 1 mM O_2^-. Potential scan rate: 50 mV s^{-1}.

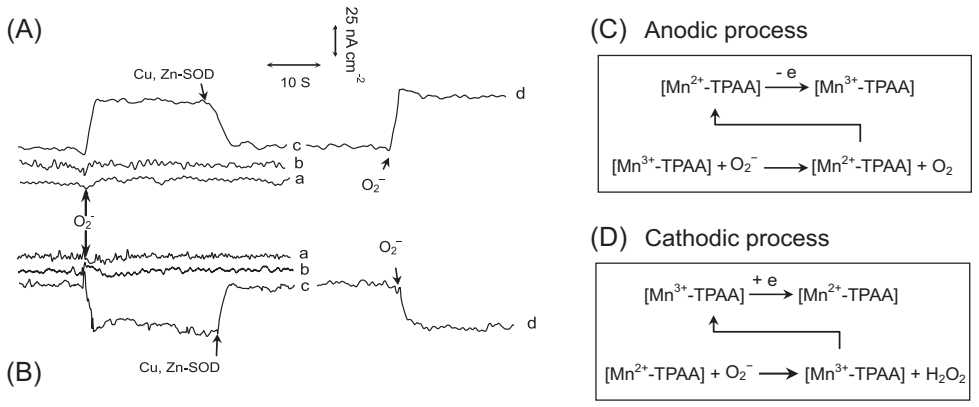

Fig. 3. Typical current–time responses obtained at (a) bare TiO_2 film, (b) TPAA/TiO_2 film, (c) Mn-TPAA/TiO_2 film in 10 mM PBS with addition of 10 μM O_2^- at (A) +650 mV and (B) 0 mV vs. Ag|AgCl, respectively. (d) Electrochemical responses obtained at the same Mn-TPAA/TiO_2 film used in (c) in the 10 mM fresh PBS with addition of 10 μM fresh O_2^- at (A) +650 mV and (B) 0 mV vs. Ag|AgCl, respectively. The arrows represent the addition of O_2^- and 0.1 mM Cu, Zn-SOD to the solution. The solution was stirred with a magnetic stirrer at 500 rpm. (C) and (D) The proposed mechanism for the anodic and cathodic process.

These observations indicate that the biomimetic activity amplifies characteristic of O_2^- oxidation or reduction at Mn-TPAA/TiO_2 electrode. More interestingly, with the addition of SOD, which is a selective scanvenger of O_2^-, the enhanced anodic or cathodic current decreased by >96%. This result demonstrates that the observed large anodic or cathodic current should be ascribed to the oxidation of $O_2^{-\bullet}$ by biomimetic electrocatalysis of Mn-TPAA, as illustrated in Fig. 3C and D. In addition, after the above tests, the current responses (d) were observed to restore at the same electrode toward fresh O_2^-. The current values are also similar to those obtained at the same electrode before the addition of SOD (c). These data confirm again that the observed current increases are ascribed to the O_2^- oxidation and reduction.

3.3. Analytical performance for O_2^- assay

By taking into account the possibility of both oxidation and reduction of O_2^- at Mn-TPAA/TiO_2 films and the formal potentials of Mn-TPAA themselves, the Mn-TPAA/TiO_2 electrodes were polarized at +650 or 0 mV vs. Ag|AgCl. Fig. 4A displays a typical amperometric response toward successive addition of O_2^- in solution at the optimized potential of either (a) +650 mV or (b) 0 mV vs. Ag|AgCl, respectively. After a stable background current was obtained under the applied potential conditions, 50 μM KO_2 was pipetted into the PBS to generate O_2^-. The introduction of KO_2 into the electrolyte solution produced a rapid and obvious increase in the anodic or cathodic current and reached the stable plateau within 6 s. Both anodic and cathodic currents increased stepwise with successive addition of O_2^- into the solution. The anodic and cathodic calibration curves were plotted in Fig. 4B. The sensitivity of Mn-TPAA/TiO_2 film was estimated to be 4.25 ± 0.12 and 3.17 ± 0.11 nA cm^{-2}/μM ($n = 9$) at +650 and 0 mV vs. Ag|AgCl, respectively. The steady-state currents at anodic and cathodic potentials were proportional to O_2^- concentration in the range of 5–225 μM and 0.2–625 μM, respectively. The wide linear detection range meets the requirement of O_2^- detection from normal physiological conditions to morbid status. The biomimetic biosensor for O_2^- based on Mn-TPAA/TiO_2 film shows wide dynamic linear range and low detection limit at the low applied potential of 0 V vs. Ag|AgCl, which is better than those O_2^- biosensors based on SOD at nanostructured gold, ZnO nanosheets, and SiC surfaces (Liu et al., 2008; Deng et al., 2008; Rafiee-Pour et al., 2010). The detection limit of the present biosensor is also a little lower than that of our previous work based on manganese (II) phosphate (Luo et al., 2009; Zhou et al., 2011). All the comparison for analytical performance was summarized in Table S1 (Supporting Information).

The selectivity of the present biosensor for O_2^- based on Mn-TPAA/TiO_2 film was also systematically examined anodically and cathodically, relative to a variety of ROS including H_2O_2, $OH^\bullet$, $ONOO^-$, $^1O_2$, and other biological substances, such as UA, DA, AA, Cys, Ca^{2+}, Na^+, K^+, Zn^{2+}, Mg^{2+}, and O_2. At +650 mV vs. Ag|AgCl, ~32.66, ~26.34, and ~21.62% current responses were obtained at Mn-TPAA/TiO_2 electrode for 5 μM DA, 10 μM AA and 5 μM Cys relative to 5 μM O_2^-, respectively. But those interferences were negligible (<2%) at applied potential of 0 mV vs. Ag|AgCl. By taking into account of both sensitivity and selectivity, the potential of 0 mV vs. Ag|AgCl was selected for determining cellular O_2^-.

For stability test, the response currents obtained at three kinds of metal-TPAA/TiO_2 electrodes for O_2^- were recorded three times daily. No significant changes (<3%) in current responses were found over a period of three months. The reproducibility was further investigated by testing the response currents for O_2^- using five independent metal-TPAA/TiO_2 electrodes. It is found that all the response variations were less than 4.8%.

3.4. Determination of extracellular O_2^- and O_2^--induced Ca^{2+} released in living cells

As demonstrated above, the present O_2^- biosensor based on Mn-TPAA/TiO_2 surface exhibits good selectivity, broad linear range, and quick response. More importantly, the biomimetic surface shows long-term stability and high reproducibility. These advantages provided a reliable and durable approach for real-time monitoring of O_2^- released from living cells. The method can also be used for determination of the relationship between O_2^- and Ca^{2+}, which may be involved in the signal transduction and other physiological and pathological events. Fig. 5A depicts amperometric responses toward extracellular O_2^- released from HeLa cells at the applied potential of 0 mV vs. Ag|AgCl (a) without and (b) with the stimulation of Ang II, since Ang II is well known to generate extracellular $O_2^{-\bullet}$ through receptor-mediated signalling cascades (Li et al., 2009; Xu et al., 2007; Tang et al., 2008; Li and Shah, 2004; Takano et al., 2002). As expected, an obvious cathodic current was observed with the stimulation of Ang II within ~25 s. However, as shown in Fig. 5B, pretreatment with NADPH oxidase inhibitor-Apo for 10 min greatly decreased the cathodic current, even with the following addition of Ang II. No obvious change of cathodic current was obtained at cells with pretreatment of anion channel blocker-DIDS for 10 min, because DIDS can only block extracellular O_2^- to transfer into

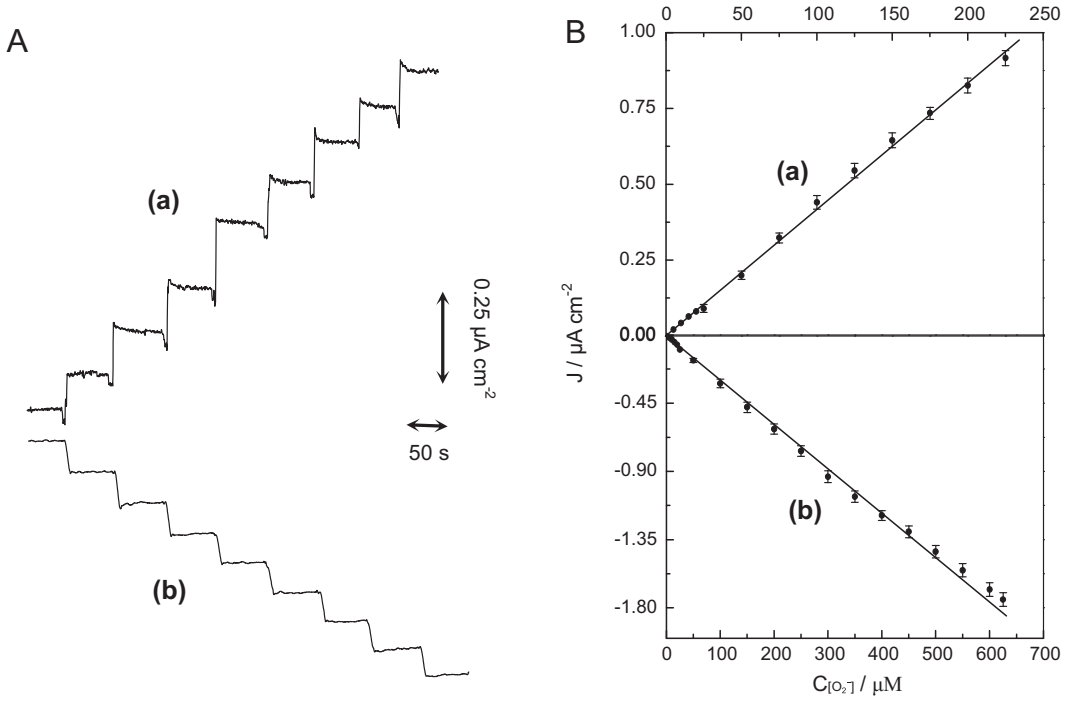

Fig. 4. (A) Amperometric responses of Mn-TPAA/TiO_2 film at applied potentials of (a) +650 mV and (b) 0 mV vs. Ag|AgCl upon successive additions of 2.5×10^{-5} M O_2^- to 10 mM PBS (pH 7.0) with stirring. The same electrode was used for both anodic and cathodic measurements. (B) Calibration plots of (a) anodic and (b) cathodic currents against concentration of O_2^-.

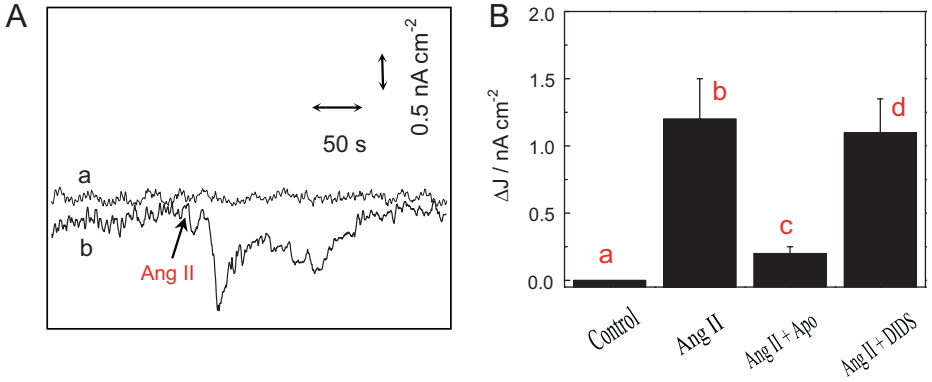

Fig. 5. (A) Amperometric responses and (B) current changes toward O_2^- released from HeLa cells stimulated (a) without Ang II or (b–d) with 2 μM Ang II, and the cells were pretreated with (c) Apo (2 μM, NADPH oxidase inhibitor) or (d) DIDS (300 μM, anion channel blocker) for 10 min. All the experiments were performed in 10 mM PBS (pH 7.4) containing 100 mM glucose at the applied potential of 0 mV vs. Ag|AgCl.

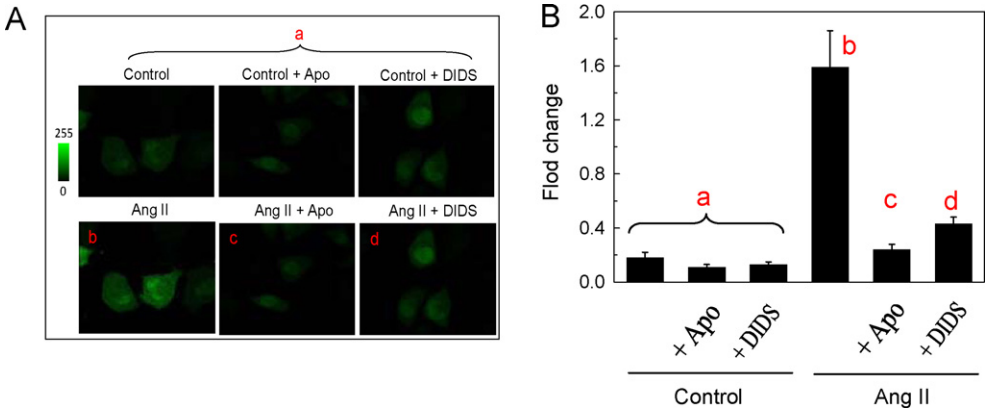

Fig. 6. Extracellular O_2^- generation results in an increase of intracellular Ca^{2+} concentration. HeLa cells loaded with Fluo 4-AM (5 μM) were stimulated (a) without or (b–d) with 2 μM Ang II, and the cells were pretreated with (c) Apo (2 μM) or (d) DIDS (300 μM) for 10 min. Fluorescent changes (D) were quantified from the confocal microscopic images (C). Quantitation was expressed as fold change vs. baseline (zero time). Data represent mean ± SD of three independent fields ($n = 3$).

the cells. These data suggest that the observed cathodic current increase is attributed to Ang II-stimulated extracellular O_2^- generation from HeLa cells. More interestingly, as shown in Fig. 6A, fluorescent intensity of cells loaded with Fluo 4-AM obviously increased with the stimulation of Ang II in the same concentration as that used in the electrochemical detection for 20 min. In addition, pretreatment with Apo or DIDS decreased the fluorescent changes of Ca^{2+} concentration in Ang II-simulated cells, indicating that the increase of intracellular Ca^{2+} concentration may be ascribed to the extracellular O_2^- generation simulated by Ang II. Fluorescent changes in Fig. 6B were quantified from the confocal microscopic images (Fig. 6A). These experimental results suggest that extracellular O_2^- across the cell membrane occurs through anion channels and induces intracellular Ca^{2+} release, which is in a good agreement with those previously reported (Li et al., 2009; Xu et al., 2007; Tang et al., 2008; Ikebuchi et al., 1991).

4. Conclusions

Mn-TPAA biomimetic enzyme has been synthesized and successfully applied to construct a reliable and durable biosensor for O_2^-. Direct electron transfer of Mn-TPAA has been realized on TiO_2 nanoneedle film with $E^{\circ\prime}$ located between the $E^{\circ\prime}$ values of the O_2/O_2^- and O_2^-/H_2O_2 redox couples, indicating that Mn-TPAA at TiO_2 films are electrochemically active and thermodynamically capable of mediating both the oxidation of O_2^- to O_2 and the reduction of O_2^- to H_2O_2. Thus, the electrochemical activities of Mn-TPAA immobilized on the TiO_2 film, together with the inherent catalytic activities of Mn-TPAA themselves toward O_2^- to form O_2 and H_2O_2, have established a reliable and durable approach for determination of O_2^- with high selectivity, broad linear range, quick response time, and so on. In addition, the biomimetic SOD-Mn-TPAA shows long-term stability, good reproducibility, and biocompatibility. Thus, the combination of good analytical performance and the advantages of biomimetic SOD opens up a new way to real-time assay of O_2^- concentration released from living cells. The as-established method has been further applied to investigate the relationship between O_2^- and Ca^{2+}, which might be related to ROS signal transduction and other physiological and pathological events. This investigation provides a methodology for constructing selective and long-term stable biosensors based on a wide variety of biomimetic enzymes.

Acknowledgments

This work was financially supported by National Natural Science Foundation of China (20975075), the National Basic Research Program of China (2010CB912604), and Nanometer Science Foundation of Shanghai (0952nm04900). Tongji University is also greatly acknowledged.

Appendix A. Supplementary data

Supplementary data associated with this article can be found, in the online version, at doi:10.1016/j.bios.2011.08.017.

References

Ai, S., Wang, Q., Li, H., Jin, L., 2005. J. Electroanal. Chem. 578, 223–229.
Bard, A.J., Parsons, R., Jordan, J., 1985. Standard Potentials in Aqueous Solution. Marcel Dekker, New York.
Barroso, M.F., de-los-Santos-Álvarez, N., Lobo-Castañón, M.J., Miranda-Ordieres, A.J., Delerue-Matos, C., Oliveira, M.B.P.P., Tuñón-Blanco, P., 2011. J. Electroanal. Chem. 659, 43–49.
Deng, Z., Rui, Q., Yin, X., Liu, H., Tian, Y., 2008. Anal. Chem. 80, 5839–5846.
Deroche, A., Morgenstern-Badarau, I., Cesario, M., Guilhem, J., Keita, B., Nadjo, L., Houée-Levin, C., 1996. J. Am. Chem. Soc. 118, 4567–4573.
Di, J., Bi, S., Zhang, M., 2004. Biosens. Bioelectron. 19, 1479–1486.
Ellis, J., Castillo, E.D., Bayon, M., Grimm, R., Clark, J.F., Pyne-Geithman, G., Wilbur, S., Caruso, J.A., 2008. J. Proteome Res. 7, 3747–3754.
Erriquez, J., Bernascone, S., Ciarletta, M., Filigheddu, N., Graziani, A., Distasi, C., 2009. Cell Calcium 46, 197–208.
Finkel, T., 2003. Curr. Opin. Cell Biol. 15, 247–254.
Floyd, R.A., 1990. FASEB J. 4, 2587–2597.
Fridovich, I., 1970. J. Biol. Chem. 245, 4053–4057.
Globus, M.Y., Alonso, O., Dietrich, W.A., Busto, R., Ginsberg, M.D., 1995. J. Neurochem. 65, 1704–1711.
Hai, C., 2006. Free Radical Medicine. The Fourth Military Medical University, Xi'an, China.
Hall, E.D., Braughler, J.M., 1989. Free Radic. Biol. Med. 6, 303–313.
Hawkins, B.J., Madesh, M., Kirkpartick, C.J., Fisher, A.B., 2007. Mol. Biol. Cell 18, 2002–2012.
Ikebuchi, Y., Masumoto, N., Tasaka, K., Koike, K., Kasahara, K., Miyake, A., Tanizawa, O., 1991. J. Biol. Chem. 266, 13233–13237.
Islam, M.M., Imase, T., Okajima, T., Takahashi, M., Niikura, Y., Kawashima, N., Nakamura, Y., Ohsaka, T., 2009. J. Phys. Chem. A 113, 912–916.
Ji, H., Li, H., Martásek, P., Roman, L.J., Poulos, T.L., Silverman, R.B., 2009. J. Med. Chem. 52, 779–797.
Komatsu, S., Yamamoto, R., Nanjo, Y., Mikami, Y., Yunokawa, H., Sakata, K., 2009. J. Proteome Res. 8, 4766–4778.
Kontos, H.A., Wei, E.P., 1986. J. Neurosurg. 64, 803–807.
Laviron, E., 1979. J. Electroanal. Chem. 101, 19–28.
Li, H., Li, Q., Wang, X., Xu, K., Chen, Z., Gong, X., Liu, X., Tong, L., Tang, B., 2009. Anal. Chem. 81, 2193–2198.
Li, J.M., Shah, A.M., 2004. Am. J. Physiol. Regul. Integr. Comp. Physiol. 287, R1014–R1030.
Liu, H., Tian, Y., Xia, P., 2008. Langmuir 24, 6359–6366.
Luo, Y., Tian, Y., Rui, Q., 2009. Chem. Commun., 3014–3016.
Lvovich, V., Scheeline, A., 1997. Anal. Chem. 69, 454–462.
Mason, R.P., Knecht, K.T., 1994. Methods Enzymol. 233, 112–127.
McCord, J.M., Fridovich, I., 1968. J. Biol. Chem. 243, 5753–5760.
McCord, J.M., Fridovich, I., 1969. J. Biol. Chem. 244, 6094–6095.
McNeil, C.J., Greenough, K.R., Weeks, P.A., Self, C.H., 1992. Free Radic. Res. Commun. 17, 399–406.
Mesároš, S., Vaňková, Ž., Grunfeld, S., Mesárošová, A., Malinski, T., 1998. Anal. Chim. Acta 358, 27–33.
Morton-Jones, R.T., Cannell, M.B., Housley, G.D., 2008. Cell Calcium 43, 356–366.
Mossine, V.V., Linetsky, M., Glinsky, G.V., Ortwerth, B.J., Feather, M.S., 1999. Chem. Res. Toxicol. 12, 230–236.
Nagano, T., Hirano, T., Hirob, M., 1989. J. Biol. Chem. 264, 9243–9249.
Ohara, Y., Peterson, T.E., Harrison, D.G., 1993. J. Clin. Invest. 91, 2546–2554.
Ohsaka, T., Tian, Y., Shioda, M., Kasahara, S., Okajima, T., 2002. Chem. Commun., 990–991.
Ohyashiki, T., Nunomura, M., Katoh, T., 1999. Biochim. Biophys. Acta 1421, 131–139.
Oritani, T., Fukuhara, N., Okajima, T., Kitamura, F., Ohsaka, T., 2004. Inorg. Chim. Acta 357, 436–442.
Rafiee-Pour, H., Noorbakhsh, A., Salimi, A., Ghourchian, H., 2010. Electroanalysis 22 (14), 1599–1606.
Sadek, H.A., Szweda, P.A., Szweda, L.I., 2004. Biochemistry 43, 8494–8502.
Shi, G., Sun, Z., Liu, M., Zhang, L., Liu, Y., Qu, Y., Jin, L., 2007. Anal. Chem. 79, 3581–3588.
Song, M., Bier, F., Scheller, F., 1995. Bioelectrochem. Bioenerg. 38, 419–422.
Takano, M., Meneshian, A., Sheikh, A., Yamakawa, Y., Wilkins, K.B., Hopkins, E.A., Bulkley, G.B., 2002. Am. J. Physiol. Heart Circ. Physiol. 283, H2054–H2061.
Tanabe, S., Wang, X., Takahashi, N., Uramoto, H., Okada, Y., 2005. FEBS Lett. 579, 517–522.
Tang, B., Zhang, N., Chen, Z., Xu, K., Zhuo, L., An, L., Yang, G.J, 2008. Chem. Eur. J. 14, 522–528.
Thomas, C.E., Bernardelli, P., Bowen, S.M., Chaney, S.F., Friedrich, D., Janowick, D.A., Jones, B.K., Keeley, F.J., Kehne, J.H., Ketteler, B., Ohlweiler, D.F., Paquette, L.A., Robke, D.J., Fevig, T.L., 1996. J. Med. Chem. 39, 4997–5004.
Tian, Y., Mao, L., Okajima, T., Ohsaka, T., 2002. Anal. Chem. 74, 2428–2434.
Tian, Y., Mao, L., Okajima, T., Ohsaka, T., 2004. Anal. Chem. 76, 4162–4168.
Tian, Y., Mao, L., Okajima, T., Ohsaka, T., 2005. Biosens. Bioelectron. 21, 557–564.
Vanella, A., Di Giacomo, C., Sorrenti, V., Russo, A., Castorina, C., Campisi, A., Renis, M., Perez-Polo, J.R., 1993. Neurochem. Res. 18, 1337–1340.
Vasquez-Vivar, J., Hogg, N., Pritchard, K.A., Kalyanaraman, B., 1997. FEBS Lett. 403, 127–130.
Wang, W., Fang, H., Groom, L., Cheng, A., Zhang, W., Liu, J., Wang, X., Li, K., Han, P., Zheng, M., Yin, J., Wang, W., Mattson, M., Kao, J., Lakatta, E., Sheu, S., Ouyang, K., Chen, J., Dirksen, R., Cheng, H., 2008. Cell 134, 279–290.
Wang, Y., Wu, Y., Wang, J., Di, J., 2009. Bioprocess Biosyst. Eng. 32, 531–536.
Wrona, M.Z., Dryhurst, G., 1998. Chem. Res. Toxicol. 11, 639–650.
Xu, K., Liu, X., Tang, B., Yang, G., Yang, Y., An, L., 2007. Chem. Eur. J. 13, 1411–1416.
Zhou, J., Luo, Y., Zhu, A., Liu, Y., Zhu, Z., Tian, Y., 2011. Analyst 136, 1594–1598.